Age of the Badenian salinity crisis; impact of Miocene climate variability on the circum-Mediterranean region

A. de Leeuw[1,*], K. Bukowski[2], W. Krijgsman[1], and K.F. Kuiper[3]

[1]Paleomagnetic Laboratory "Fort Hoofddijk," Faculty of Geosciences, Utrecht University, Budapestlaan 17, 3584 CD Utrecht, Netherlands

[2]Faculty of Geology, Geophysics and Environmental Protection, AGH University of Science and Technology, A. Mickiewicza 30, 30-059 Krakow, Poland

[3]Faculty of Earth and Life Sciences, Institute of Earth Sciences, Vrije Universiteit Amsterdam, De Boelelaan 1085, 1081 HV Amsterdam, Netherlands

ABSTRACT

Massive evaporites were deposited in the Central European Paratethys Sea during the Badenian salinity crisis (BSC). The scarcity of absolute age data has hampered a thorough understanding of these salt deposits. Here we present a robust chronology for this catastrophic event by $^{40}Ar/^{39}Ar$ dating of volcanic tuffs below and within the Badenian salts in southern Poland. The onset of BSC evaporite deposition is dated at 13.81 ± 0.08 Ma and the entire event is estimated to have lasted 200–600 k.y. Correlation to oxygen isotope records shows that the BSC evaporites were just preceded by glacial event Mi-3b, suggesting a causal relationship. The corresponding sea-level fall most likely restricted the open marine connection to the Mediterranean, thereby trapping the salt in the deep Paratethys basins.

INTRODUCTION

The circum-Mediterranean Miocene was marked by several occurrences of extraordinary paleoenvironmental catastrophes, during which large water masses were cut off from the open ocean, resulting in the formation of hypersaline waters, complete destruction of biological ecosystems, and deposition of giant (100–1000 m) evaporite units in the deep as well as marginal basins. These so-called salinity crises occurred in the Middle Miocene (ca. 15 Ma) of the Red Sea (e.g., Rouchy et al., 1995), the Late Miocene (ca. 6 Ma) of the Mediterranean (e.g., Hsü et al., 1973), and the Badenian (ca. 14 Ma) of the Paratethys (e.g., Peryt, 2006), the larger precursor of the Black Sea, and are commonly considered to have been caused by a complex interplay of tectonic and glacio-eustatic processes that resulted in progressive closure of the marine gateways, and hence in the obstruction of the hydrological exchange between different basins.

An accurate chronostratigraphic framework is a key prerequisite for the correct deciphering of evaporite basin evolution, as demonstrated for the Messinian salinity crisis of the Mediterranean (Krijgsman et al., 1999; Roveri et al., 2008). In this paper we focus on constructing a reliable chronology for the Badenian salinity crisis (BSC) by isotopic ($^{40}Ar/^{39}Ar$) dating of volcanic tuff layers located directly below and within the Badenian halite units of the northern Carpathian foredeep in southern Poland (Fig. 1). The new data help to distinguish between tectonic and paleoclimatic causes and to elaborate on the progression of evaporite formation in these highly restricted environments.

BSC OF THE PARATETHYS

The Badenian stage marks the last period of significant connectivity between the Mediterranean and Paratethys. The only postulated seaway was situated in the narrow area between the Alps and the Dinarids (Fig. 1) that progressively decreased during the lower Badenian by a combination of tectonic and glacio-eustatic processes (Rögl, 1998). This resulted in the formation of massive salt deposits in the Central European Paratethys basins.

The Badenian evaporites of southern Poland are 30–100 m thick and consist of Ca-sulfates (anhydrite and gypsum) or halite with intercalations of claystones and minor Ca-sulfates. Sulfates occur in a broad belt along the northern and the central parts of the Carpathian foredeep and its foreland. Halite is limited to a small area along the northern rim of the Carpathians (Fig. 1). The halite is commonly underlain by deep-marine siliciclastics and carbonates (Skawina Beds) and overlain by deep-marine to brackish siliciclastic deposits (Chodenice and Gliwice Beds) (Porębski et al., 2003; Peryt, 2006). Facies analyses suggest that the deep Badenian evaporites originated from density-stratified brines (Garlicki, 1979; Bąbel, 1999). Halite precipitation commenced in the deepest parts of the basin where the heaviest brines occurred, and slightly predated the onset of Ca-sulfates at the basin margins (Peryt, 2006).

Based on the absence of the nannofossil *Sphenolithus heteromorphus*, the base of the Badenian evaporites was correlated to nannoplankton zone NN6 (Peryt, 1997), corresponding to the time interval of ca. 13.65–13.0 Ma (Lourens et al., 2004). This was supported by K-Ar dating of the tuff horizon (WT-3) occurring below the salt in southern Poland (Fig. 1) that gave an age of 13.6 ± 0.2 Ma (Dudek et al., 2004), although the $^{40}Ar/^{39}Ar$ age for the same tuff was 12.0 ± 0.3 Ma (Bukowski et al., 2000).

RADIOISOTOPE DATING

We decided to redate the key volcanic ashes of the Polish successions by the $^{40}Ar/^{39}Ar$ method to better understand the processes underlying the BSC. Two tuff layers (WT-1 and WT-3) were sampled in the historical (exploited during more than seven centuries) salt mines in Wieliczka and Bochnia (Bukowski, 1999; Dudek et al., 2004). WT-1 is located a few meters below the first halite deposits, while WT-3 is found in the middle part of the halite unit. The $^{40}Ar/^{39}Ar$ ages (Table 1) of the hornblende (WT-1) and biotite (WT-3) separates obtained from these layers were determined applying (standard)

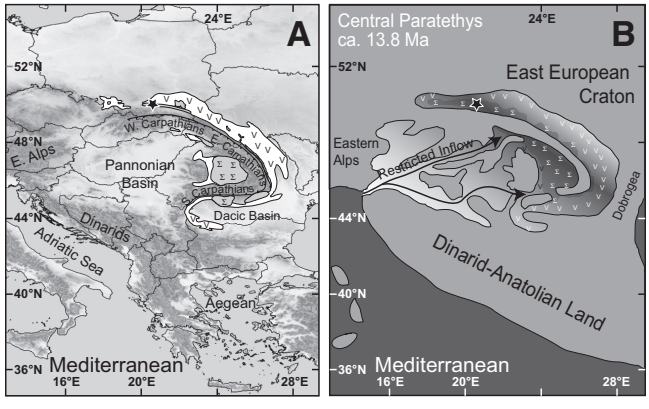

Figure 1. A: Facies map displaying distribution of halite (Σ) and gypsum and/or anhydrite (V) deposits along Carpathians. B: Simplified paleogeographic reconstruction of Mediterranean-Paratethys connection during Badenian salinity crisis interval (modified after Rögl, 1998). Star marks location of studied section.

*E-mail: adeleeuw@geo.uu.nl.

incremental heating techniques (see the GSA Data Repository[1]). Ages were calculated using the recalibrated Fish Canyon Tuff sanidine neutron flux monitor age of 28.20 ± 0.03 Ma (Kuiper et al., 2008), thereby allowing direct comparison to astronomically dated geological records. Results are displayed as age spectra diagrams (Fig. 2). Duplicate measurements provided plateau ages of 13.78 ± 0.04 and 13.83 ± 0.04 Ma for WT-1. Plateau ages for the two WT-3 duplicates amount to 13.58 ± 0.01 and 13.61 ± 0.02 Ma. None of the inverse isochron intercepts deviates from the value of atmospheric argon. We arrive at a weighted mean age of 13.81 ± 0.03 Ma for WT-1 and 13.60 ± 0.01 Ma for WT-3: errors increase to 0.08 and 0.07 Ma respectively, if the uncertainties in standard age and decay constants are included (see the Data Repository). All errors are quoted at the 1σ level.

ONSET OF THE BSC

Reliable chronologic data provide better means to discriminate between climatic and tectonic processes by direct correlation to the global oxygen isotope records and astronomical target curves. Our $^{40}Ar/^{39}Ar$ results indicate that evaporite deposition in the Carpathian foredeep started shortly after 13.81 ± 0.08 Ma. This indicates that the BSC took place simultaneously with or directly after Mi3b (Fig. 3), the major step in Middle Miocene global cooling dated at 13.82 ± 0.03 Ma in the Mediterranean (Abels et al., 2005), and clearly expressed in many isotope records worldwide (e.g., Holbourn et al., 2005). A significant decline in temperature has also been documented from below the evaporites by the displacement of warm-water planktonic foraminiferal assemblages and the expansion of the cool-water populations (Gonera et al., 2000; Bicchi et al., 2003). Harzhauser and Piller (2007) indicated that the mid-Badenian extinction event, a sharp decline in the number of gastropod and foraminifera taxa that characterizes evaporite-free Paratethys successions coeval with the BSC, coincided with a decline in the share of thermophilous mollusc taxa. This indicates a drop in sea-surface temperature from 16–18 °C to 14–15 °C. A causal relationship between the Mi3b cooling event and the BSC thus seems likely. At first sight, it is counterintuitive that evaporites form under colder climatic circumstances, because these would principally lead to less evaporation. The BSC, however, was preceded by such an intense climatic optimum (Böhme, 2003) that the hydrological budget (precipitation – evaporation) remained negative, directly after the cooling event.

In the early and middle Badenian, and thus during the BSC, the circulation in the Central Paratethys was anti-estuarine (Baldi, 2006). The Mi3b cooling step triggered a significant drop (~40–50 m) in global sea level (John et al., 2004; Westerhold et al., 2005) that deteriorated the water exchange through the gateway to the Mediterranean. Model results show that under negative hydrological budgets salinity will rise if the connecting strait is sufficiently shallow (Meijer and Krijgsman, 2005). While changes in precipitation patterns at low and

TABLE 1. SUMMARY OF THE $^{40}Ar/^{39}Ar$ RESULTS

Sample	Mineral	J-value	Plateau age (Ma)	Analytical error	Total error	MSWD	N(n)	$^{40}Ar^{*}$ (%)	^{39}A (%)	K/Ca	Inverse isochron intercept
WT-1 1	hornblende	0.0026848	13.83	0.04	0.08	0.51	16(10)	89.45	93.86	0.071 ± 0.001	297.0 ± 15.7
WT-1 2	hornblende	0.0026848	13.78	0.04	0.08	0.72	17(10)	90.38	91.69	0.071 ± 0.001	322.5 ± 14.3
WT-1 combined	hornblende	0.0026848	13.81	0.03	0.08	0.61	33(20)	89.91	92.82	0.071 ± 0.001	312.9 ± 10.6
WT-3 1	biotite	0.002685	13.58	0.01	0.07	0.75	16(8)	93.98	68.82	39.499 ± 4.404	335.1 ± 36.0
WT-3 2	biotite	0.002685	13.61	0.02	0.07	0.7	16(7)	94.48	67.77	52.865 ± 8.699	368.6 ± 74.5
WT-3 combined	biotite	0.002685	13.60	0.01	0.07	0.82	32(15)	94.21	68.08	43.886 ± 4.469	337.1 ± 31.9

Note: J-value—irradiation parameter; MSWD—mean square of weighted deviates; N—number of increments measured during the incremental heating experiment; n—number of increments included in the plateau.

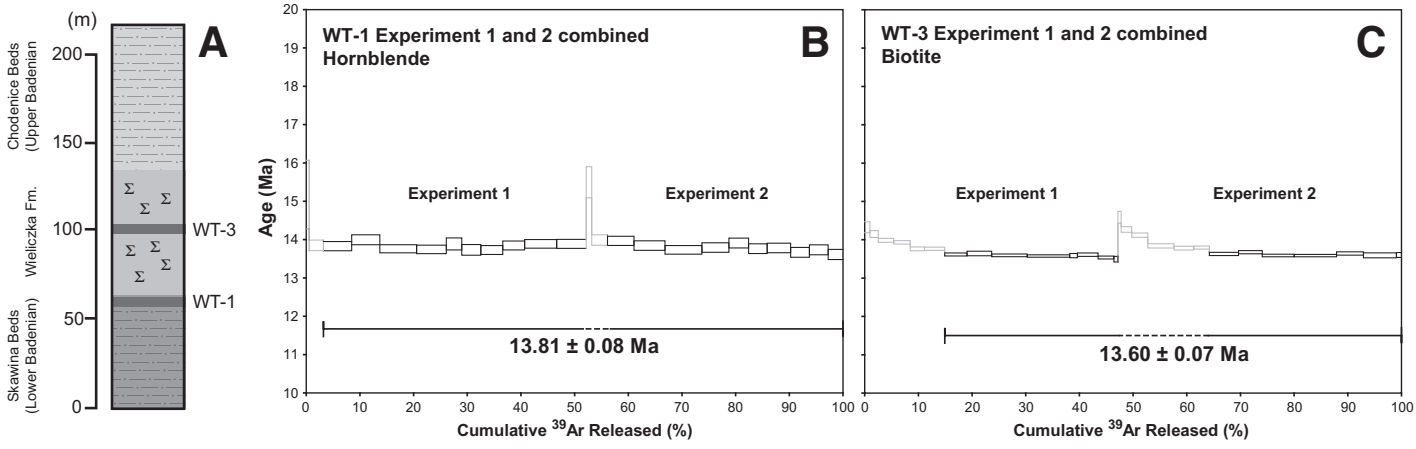

Figure 2. A: Generalized stratigraphic column for Carpathian foredeep near Wieliczka salt mine. Stratigraphic positions of halite (Σ) and sampled volcanic tuffites (WT-1 and WT-3) are indicated. B: Age spectra diagram for WT-1 tuff layer with chosen plateaus (steps indicated in blue) and their weighted ages. C: WT-3. Duplicate measurements were performed for each of two tuffs. Final ages of WT-1 and WT-3 are calculated on basis of combined weighted plateaus of these duplicate measurements. Depicted overall uncertainty includes analytical error as well as external uncertainties. For individual steps in plateau, only analytical uncertainty is given, indicated by thickness of blocks representing individual steps (see the Data Repository [see footnote 1]).

[1]GSA Data Repository item 2010197, description of the $^{40}Ar/^{39}Ar$ dating procedure and Tables DR1–DR6 (analytical data), is available online at www.geosociety.org/pubs/ft2010.htm, or on request from editing@geosociety.org or Documents Secretary, GSA, P.O. Box 9140, Boulder, CO 80301, USA.

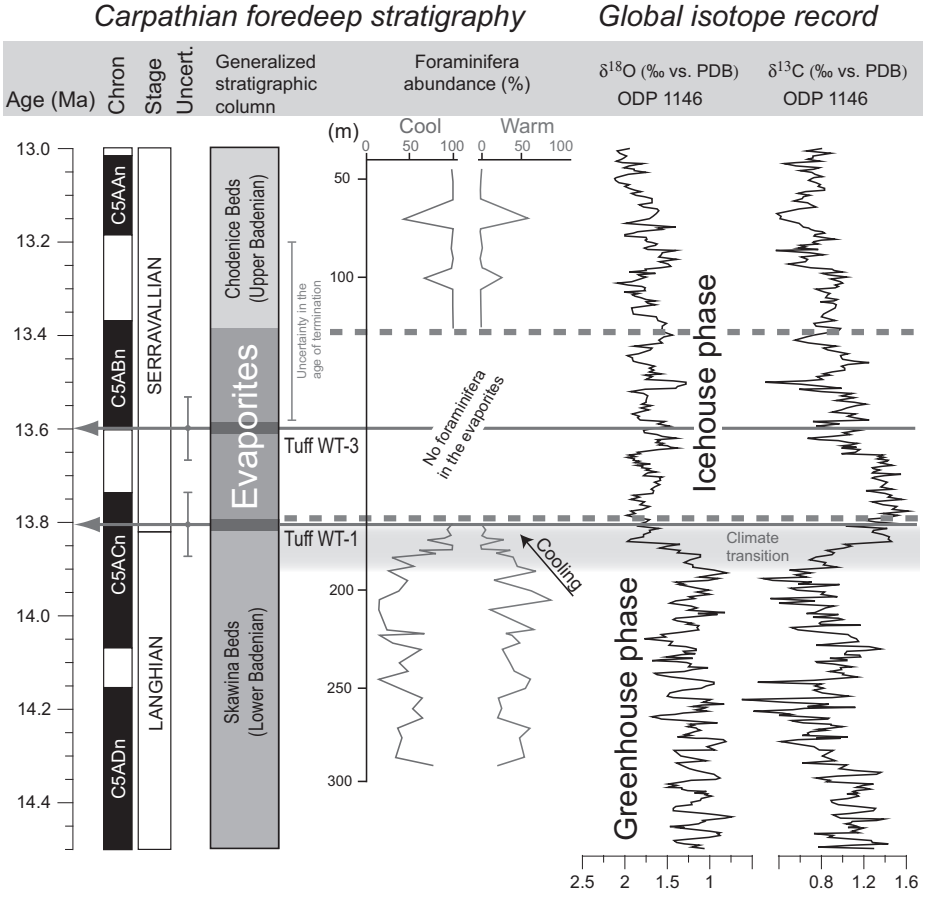

Figure 3. Detailed correlation figure showing chronostratigraphic position of Wieliczka halite deposits. Badenian salinity crisis coincides with start of Miocene icehouse period. Foraminifera assemblages in drill core Gliwice 19 indicate cooling just before deposition of evaporites (data from Bicchi et al., 2003). Stable oxygen and carbon isotope data from Ocean Drilling Program (ODP) Site 1146 in Caribbean (Holbourn et al., 2007) show Middle Miocene global climate transition with its major step, Mi3b, at 13.82 Ma. Ages of magnetic chrons are from Lourens et al. (2004) with adjustments according to Hüsing et al. (2010). Position of Langhian-Serravallian boundary is from Abels et al. (2005). PDB—Peedee belemnite.

middle latitudes accompanying the global drop in temperature might have stimulated evaporite formation in Central Europe, the Mi3b sea-level lowering most likely played a crucial role in the onset of the BSC. It restricted the deep outflow of dense saline waters from the Carpathian foredeep, trapped the salt within the Paratethys basins, and consequently set off the BSC.

The Mi3b event furthermore coincided with minimum eccentricity values associated with the 400 k.y. cycle and minimum obliquity amplitudes associated with the 1.2 m.y. cycle (Abels et al. 2005). It implies that this specific orbital configuration indirectly triggered the BSC, thereby providing an extreme example of the influence of long-period astronomical cyclicity on the paleoenvironment.

PROGRESSION AND TERMINATION OF THE BSC

The difference in age between volcanic tuffs WT-1 and WT-3 is 210 ± 32 k.y. Because all samples were co-irradiated side by side and measured consecutively in the same setup, the uncertainty in the age difference (or duration) is much lower than the uncertainty in the absolute age of the individual volcanic ashes, since we do not need to take into account uncertainties in standard ages and decay constants. Assuming the upper half of the evaporites was deposited in a similar time span as the lower half, the total package would be deposited in ~400 k.y. Taking uncertainties in the stratigraphic position of WT-3 and potential changes in sedimentation rate into account, we estimate the total duration of evaporite deposition as 200–600 k.y. Although we realize this is only a rough first-order approximation, it is the best estimate on the basis of isotopic age data currently available. The BSC was previously suggested to comprise only 20–35 k.y., based on observations of cyclic centimeter-scale laminae within the Ca-sulfate and halite deposits, under the assumption that these represent annual accumulations (Peryt, 2006). Our results indicate that the observed cyclicity is of ~10–30 yr, implying a driving mechanism different from seasonality. The 11 yr sunspot cycle is a potential external forcing factor. Internal forcing could result from autocyclic behavior in regional climate systems, nowadays evident in, e.g., the El Niño–Southern Oscillation and North Atlantic Oscillation. The laminae could furthermore represent storm events that often have a recurrence interval of several years (e.g., Peryt, 2006).

Even though only a rough age estimate for the end of the BSC can be derived, the newly acquired $^{40}Ar/^{39}Ar$ ages do not support a glacio-eustatic cause, since after 13.82 Ma global climate gradually deteriorated and sea level did not rise significantly. The termination of the BSC is thus most likely related to a tectonically driven transgression, resulting in the dilution of brines by inflowing marine water (e.g., Krzywiec, 2001; Baldi, 2006). The circulation pattern in the Central Paratethys changed to estuarine, which might have enhanced the cooling of Central Europe (Baldi, 2006). Many authors envisage a new connection to the Indian Ocean, due to the presence of Indo-Pacific elements in the late Badenian fauna (e.g., Rögl, 1998). This hydrological change must have taken place in a relatively short time span, because the basin water rapidly gained normal salinity.

COMPARISON TO THE MESSINIAN SALINITY CRISIS OF THE MEDITERRANEAN

The BSC was not a unique event in the circum-European region. The Mediterranean Sea underwent an even more dramatic crisis when it became progressively isolated from the Atlantic Ocean during the Messinian (e.g., Hsü et al., 1973; Rouchy and Caruso, 2006). The Messinian salinity crisis, astronomically dated between 5.96 and 5.33 Ma (Krijgsman et al., 1999), generated more than 1000 m of salt in the deep Mediterranean basins. The 630 k.y. duration of the Messinian salinity crisis is about the same as that of the BSC, although Messinian salinity crisis halite deposition lasted at most ~80 k.y. (Krijgsman and Meijer, 2008). The Messinian salinity crisis halites also have a cyclic laminated character, similar to the BSC evaporites (e.g., Roveri et al., 2008). This indicates that sub-Milankovitch forcing is an important component in Miocene climate evolution and especially evident during evaporite deposition. The timing of the Messinian salinity crisis does not coincide with a major glacio-eustatic sea-level fall (Hodell et al., 2001). Tectonic restriction of the sea strait to the Atlantic Ocean and consequent blocking of the inflow of normal marine water is thus its most likely cause. It follows that the Messinian salinity crisis and BSC are two end-member types in terms of the mechanism of gateway restriction; tectonic sill uplift, and eustatic sea-level lowering.

While tectonic sill uplift provided the right conditions, the exact timing of the Messinian salinity crisis may well have been controlled by the 400 k.y. component of the Earth's eccentricity cycle (Krijgsman et al., 1999). For the BSC, the trigger was a drop in sea level provoked by coincident minima in the long-period astronomical cycles. This suggests that these orbital cycles exert a large influence on these semi-isolated basins and were a key factor in the initiation of salinity crises in the (circum-)Mediterranean area.

CONCLUSIONS

Our newly acquired $^{40}Ar/^{39}Ar$ ages indicate that the evaporites of the BSC were deposited shortly after 13.81 ± 0.08 Ma, suggesting they were triggered by the worldwide cooling event Mi3b. Sea-level lowering induced by this main step in the Middle Miocene climate transition most likely restricted the already narrow straits connecting the Paratethys basin to the world's oceans. Due to preferential blockage of the deep saline outflow, salt could accumulate, eventually leading to brine formation and start of the BSC. Evaporite formation lasted 200–600 k.y. before incipient tectonism permitted normal marine water into the basins, which diluted the salt-precipitating brines. Since both the BSC and the Messinian salinity crisis were likely indirectly triggered by a specific orbital configuration, they represent extreme examples of the influence long-period astronomical cycles had on the paleoenvironment.

ACKNOWLEDGMENTS

We thank Roel van Elsas for assistance with mineral separation and Jan Wijbrans for discussion. This research was supported by the Netherlands Research Centre for Integrated Solid Earth Sciences (ISES) and by the Netherlands Organization for Scientific Research (NWO/ALW). We thank three anonymous reviewers for comments that significantly improved the manuscript.

REFERENCES CITED

Abels, H.A., Hilgen, F.J., Krijgsman, W., Kruk, R.W., Raffi, I., Turco, E., and Zachariasse, W.J., 2005, Long-period orbital control on middle Miocene global cooling: Integrated stratigraphy and astronomical tuning of the Blue Clay Formation on Malta: Paleoceanography, v. 20, no. 4, p. 1–17, doi: 10.1029/2004PA001129.

Bąbel, M., 1999, History of sedimentation of the Nida Gypsum deposits (middle Miocene, Carpathian Foredeep, southern Poland): Geological Quarterly, v. 43, p. 429–448.

Báldi, K., 2006, Paleoceanography and climate of the Badenian (Middle Miocene, 16.4–13.0 Ma) in the Central Paratethys based on foraminifera and stable isotope ($\delta^{18}O$ and $\delta^{13}C$) evidence: International Journal of Earth Sciences, v. 95, p. 119–142.

Bicchi, E., Ferrero, E., and Gonera, M., 2003, Palaeoclimatic interpretation based on Middle Miocene planktonic foraminifera: The Silesia Basin (Paratethys) and Monferrato (Tethys) records: Palaeogeography, Palaeoclimatology, Palaeoecology, v. 196, p. 265–303, doi: 10.1016/S0031-0182(03)00368-7.

Böhme, M., 2003, The Miocene climatic optimum: Evidence from ectothermic vertebrates of central Europe: Palaeogeography, Palaeoclimatology, Palaeoecology, v. 195, p. 389–401, doi: 10.1016/S0031-0182(03)00367-5.

Bukowski, K., 1999, Porównanie badeńskiej serii solonośnej z Wieliczki I Bochni w świetle nowych danych: Prace Państwowego Instytutu Geologicznego, v. 58, p. 43–56.

Bukowski, K., Galamay, A.R., and Góralski, M., 2000, Inclusion brine chemistry of the Badenian salt from Wieliczka: Journal of Geochemical Exploration, v. 69, p. 87–90, doi: 10.1016/S0375-6742(00)00118-7.

Dudek, K., Bukowski, K., and Wiewiórka, J., 2004, Datowanie radiometryczne badeńskich osadów piroklastycznych z okolic Wieliczki i Bochni: Kraków, Materiały VIII Ogólnopolskiej Sesji Naukowej "Datowanie Minerałów i Skał ", p. 18–19.

Garlicki, A., 1979. Sedymentacja soli mioceńskich w Polsce: Prace Geologiczne, no 119, p. 1–66 (in Polish with English summary).

Gonera, M., Peryt, T.M., and Durakiewicz, T., 2000, Biostratigraphical and palaeoenvironmental implications of isotopic studies (^{18}O, ^{13}C) of middle Miocene (Badenian) foraminifers in the Central Paratethys: Terra Nova, v. 12, p. 231–238, doi: 10.1046/j.1365-3121.2000.00303.x.

Harzhauser, M., and Piller, W.E., 2007, Benchmark data of a changing sea—Palaeogeography, palaeobiogeography and events in the Central Paratethys during the Miocene: Palaeogeography, Palaeoclimatology, Palaeoecology, v. 253, p. 8–31.

Hodell, D.A., Curtis, J.H., Sierro, F.J., and Raymo, M.E., 2001, Correlation of late Miocene to early Pliocene sequences between the Mediterranean and North Atlantic: Paleoceanography, v. 16, p. 164–178, doi: 10.1029/1999PA000487.

Holbourn, A.E., Kuhnt, W., Schulz, M., and Erlenkeuser, H., 2005, Impacts of orbital forcing and atmospheric CO_2 on Miocene ice-sheet expansion: Nature, v. 438, p. 483–487, doi: 10.1038/nature04123.

Holbourn, A., Kuhnt, W., Schulz, M., Flores, J.A., and Andersen, N., 2007, Orbitally-paced climate evolution during the middle Miocene "Monterey" carbon-isotope excursion: Earth and Planetary Science Letters, v. 261, p. 534–550, doi: 10.1016/j.epsl.2007.07.026.

Hsü, K.J., Ryan, W.B.F., and Cita, M.B., 1973, Late Miocene desiccation of the Mediterranean: Nature, v. 242, p. 240–244, doi: 10.1038/242240a0.

Hüsing, S.K., Cascella, A., Hilgen, F.J., Krijgsman, W., Kuiper, K.F., Turco, E., and Wilson, D., 2010, Astrochronology of the Mediterranean Langhian between 15.29 and 14.17 Ma: Earth and Planetary Science Letters, v. 290, p. 254–269, doi: 10.1016/j.epsl.2009.12.002.

John, C.M., Karner, G.D., and Mutti, M., 2004, $\delta^{18}O$ and Marion Plateau backstripping: Combining two approaches to constrain late middle Miocene eustatic amplitude: Geology, v. 32, p. 829–832, doi: 10.1130/G20580.1.

Krijgsman, W., and Meijer, P.T., 2008, Depositional environments of the Mediterranean "Lower Evaporites" of the Messinian salinity crisis: Constraints from quantitative analyses: Marine Geology, v. 253, p. 73–81, doi: 10.1016/j.margeo.2008.04.010.

Krijgsman, W., Hilgen, F.J., Raffi, I., Sierro, F.J., and Wilson, D.S., 1999, Chronology, causes and progression of the Messinian salinity crisis: Nature, v. 400, p. 652–655, doi: 10.1038/23231.

Krzywiec, P., 2001, Contrasting tectonic and sedimentary history of the central and eastern parts of the Polish Carpathian foredeep basin—Results of seismic data interpretation: Marine and Petroleum Geology, v. 18, p. 13–38, doi: 10.1016/S0264-8172(00)00037-4.

Kuiper, K.F., Deino, A., Hilgen, F.J., Krijgsman, W., Renne, P.R., and Wijbrans, J.R., 2008, Synchronizing rock clocks of Earth history: Science, v. 320, no. 5875, p. 500, doi: 10.1126/science.1154339.

Lourens, L.J., Hilgen, F.J., Shackleton, N.J., Laskar, J., and Wilson, D., 2004, The Neogene period, *in* Gradstein, F.M., et al., A geologic time scale 2004: Cambridge, Cambridge University Press, p. 409–440.

Meijer, P.T., and Krijgsman, W., 2005, A quantitative analysis of the desiccation and re-filling of the Mediterranean during the Messinian Salinity Crisis: Earth and Planetary Science Letters, v. 240, p. 510–520, doi: 10.1016/j.epsl.2005.09.029.

Peryt, D., 1997, Calcareous nannoplankton stratigraphy of the Middle Miocene in the Gliwice area (Upper Silesia, Poland): Polish Academy of Sciences Bulletin, Earth Sciences, v. 45, p. 119–131.

Peryt, T.M., 2006, The beginning, development and termination of the Middle Miocene Badenian salinity crisis in Central Paratethys: Sedimentary Geology, v. 188, p. 379–396, doi: 10.1016/j.sedgeo.2006.03.014.

Porębski, S., Pietsch, K., Hodiak, R., and Steel, R., 2003, Origin and sequential development of Badenian-Sarmatian clinoforms in the Carpathian foreland basin (SE Poland): Geologica Carpathica Clays, v. 54, no. 2, p. 119–136.

Rögl, F., 1998, Palaeogeographic considerations for Mediterranean and Paratethys seaways (Oligocene to Miocene): Annalen des Naturhistorischen Museums in Wien, v. 99, p. 279–310.

Rouchy, J.M., and Caruso, A., 2006, The Messinian salinity crisis in the Mediterranean basin: A reassessment of the data and an integrated scenario: Sedimentary Geology, v. 188, p. 35–67, doi: 10.1016/j.sedgeo.2006.02.005.

Rouchy, J.M., Noel, D., Wali, A.M.A., and Aref, M.A.M., 1995, Evaporitic and biosiliceous cyclic sedimentation in the Miocene of the Gulf of Suez—Depositional and diagenetic aspects: Sedimentary Geology, v. 94, p. 277–297, doi: 10.1016/0037-0738(94)00095-C.

Roveri, M., Lugli, S., Manzi, V., and Schreiber, B.C., 2008, The Messinian Sicilian stratigraphy revisited: New insights for the Messinian salinity crisis: Terra Nova, v. 20, p. 483–488, doi: 10.1111/j.1365-3121.2008.00842.x.

Westerhold, T., Bickert, T., and Röhl, U., 2005, Middle to late Miocene oxygen isotope stratigraphy of ODP Site 1085 (SE Atlantic): New constrains on Miocene climate variability and sea-level fluctuations: Palaeogeography, Palaeoclimatology, Palaeoecology, v. 217, p. 205–222, doi: 10.1016/j.palaeo.2004.12.001.

Manuscript received 20 December 2009
Revised manuscript received 5 March 2010
Manuscript accepted 8 March 2010

Printed in USA